SEMARAK ILMU PUBLISHING

Journal of Advanced Research in Applied Mechanics

Journal homepage:
https://semarakilmu.com.my/journals/index.php/appl_mech/index
ISSN: 2289-7895

Optimization of Topology and Mechanical Properties of 3D Printed Hollow and Thin-Walled Structures via Integration of Taguchi Method and Grey Relational Analysis

Zulkarnain Abdul Latiff[1], Nik Mizamzul Mehat[2,*], Nur 'Aliya Azzahra Abdul Rauf[2], Shahrul Kamaruddin[3]

[1] Manufacturing Section, Universiti Kuala Lumpur Malaysian Spanish Institute, Kulim Hi-Tech Park, 09000 Kulim, Kedah, Malaysia
[2] Faculty of Mechanical Engineering Technology, Universiti Malaysia Perlis, Kampus UniCITI Alam, Sungau Chuchuh, 02100, Padang Besar, Perlis, Malaysia
[3] Mechanical Engineering Department, Universiti Teknologi PETRONAS, 32610, Bandar Seri Iskandar, Perak, Malaysia

ARTICLE INFO

Article history:
Received 16 November 2023
Received in revised form 12 January 2024
Accepted 26 January 2024
Available online 22 March 2024

Keywords:
PLA, 3D Printing, Taguchi Method, Grey Relational Analysis, Topology

ABSTRACT

Fused deposition modelling (FDM) as one of 3D printing technique allow for the layer-by-layer construction of objects from a CAD file using a variety of different materials. The process has become quicker and more versatile as a result of technological innovation. In this study, the Taguchi method and Grey Relational Analysis (GRA) were integrated to examine the mechanical performance and topology optimisation of polylactic acid (PLA) 3D printed hollow and thin-walled structures by FDM. The results showed that the optimized factors for the 3D printed part were identified as topology design (hexagonal), wall thickness (2 mm), layer height (0.2 mm), infill density (20%), infill layer thickness (0.6 mm), infill flow (80%), infill pattern (Triangle), print speed (100 mm/s), printing temperature (210°C), bed temperature (65°C), and orientation direction (flat along the Y-axis). The compression properties of the 3D printed part particularly for maximum force, maximum stress and compression modulus were improved by 15.42%, 66.62% and 68.61% respectively after the optimization.

1. Introduction

In recent years, 3D printing (3DP) has emerged as a revolutionary technology that has transformed the realms of manufacturing, design, and innovation. This remarkable technology, also known as additive manufacturing (AM), enables the creation of 3D objects by layering material one slice at a time directly from computer-aided design (CAD) drawings, offering unprecedented versatility and precision [1]. The development of 3DP technology has been incredibly inventive and adaptable. Its applications span across various industries, from aerospace, automotive, agriculture and healthcare to art and education, making it a topic of significant interest for researchers worldwide [2]. 3DP has emerged as a result of the need for quicker product development times and

* *Corresponding author.*
E-mail address: nikmizamzul@unimap.edu.my

https://doi.org/10.37934/aram.115.1.1835

shorter product life cycles, which will help industries stay competitive in the market [3]. Currently, the 3DP technique is able to print conventional thermoplastics, ceramics, materials based on graphene, and metal [4]. Utilizing 3DP technology will speed up production while cutting costs. The consumer's demand will also have more of an impact on production at the same time. Customers might request that a product be created according to their specifications and have a greater say in the final result, which saves both energy and time [5]. 3DP has advantages over traditional manufacturing processes in terms of resource efficiency, part flexibility, material flexibility, and production flexibility. Due of its additive nature, 3DP can utilise raw materials effectively with little loss [6].

As technology continues to advance, various techniques of 3DP have been created with various purposes allow for the production of intricate and complex shapes with precision and repeatability including stereolithography (SLA), selective laser sintering (SLS), digital light processing (DLP), binder jetting, electron beam melting (EBM), etc. Among the different 3DP techniques, fused deposition modelling (FDM) technology is the most prevalent. FDM was created in the early 1990's and employs polymer as its primary material. FDM uses heated thermoplastic filament that is extruded to manufacture parts layer by layer from the bottom to the top [7]. This 3DP technique is popular due to its ease of use and the availability of raw materials, quick cycle time, high dimensional precision, desktop capability, and safety but also, because it allows the addition of reinforcement fibres continuously during the manufacturing process of the parts. FDM may also be easily integrated with a variety of CAD programs [8]. In FDM 3D printing the head of the printer is moving in X and Y axes and the up and down movement is done by the bed (Z-axis). The printer head contains a heater (extruder), the filament is fed through the heater, then it is deposited from a nozzle in a semi-molten state. The movement of the head and the flatbed is controlled easily by microcontrollers that move the motors, and the relative movement between them is set from the slicing software. At first, the printer creates the model in 2D shape, and then the bed shifts downward to increase the gap between the nozzle's tip and the bed to deposit the next layer. This procedure is repeated until the machine makes the whole 3D model [9]. Table 1 shows the usage of plastic materials in additive manufacturing.

Table 1
Plastic uses in Additive Manufacturing (AM) (Rouse 2022)

SLA	SLS	DLP	FDM
Epoxy-acrylates	Polyamide 12	PLA	PLA
Acrylates-methacrylate	Polyamide 11	PETG	ABS
	Glass fibre filled		PC
Urethane-acrylates			PETG

Despite the fact that FDM is a widely utilized and effective techniques, it has restricted uses due to its compatibility with only specified materials. Due to their melting temperature and ease of printing, polymeric materials have been preferred over other materials for processing 3D printed parts under the FDM technique. Poly Lactic Acid (PLA), Poly Carbonate (PC), Acrylonitrile Butadiene Styrene (ABS), Poly-Ether-Ether-Ketone (PEEK) are examples of the common polymeric materials used in FDM. PLA is one of the most favourable polymeric materials used in FDM due to its low melting temperature, biodegradability, and ease of printing [10]. PLA is a biodegradable thermoplastic derived from completely renewable resources like corn, sugarcane, wheat, or other high-carbohydrate resources making it environmentally friendly [11]. In contrast to other plastics, which have presented significant disposal issues, PLA plastics are compostable and decompose swiftly when disposed of. When exposed to natural circumstances, hydrolysis, or even burning, PLA

degrades to water, biomass, inorganic salts, natural and non-toxic gases, and water [12]. However, PLA is reported more brittle compared to some other 3D printing materials, especially when printed with thin walls structures. This makes it susceptible to cracking or breaking under stress or impact, limiting its use in applications requiring high durability [13].

Thin-walled structures are key elements in many industrial domains such as aircraft, shipbuilding, bridges, industrial buildings, pipelines, and others. Thin wall structures are used to produce lightweight components like brackets, supports, and panels in the aerospace industry, reducing the overall weight of aircraft and spacecraft [14]. In the FDM technique, developing a 3D model of hollow and thin-walled structures using PLA is quiet challenging. There are numbers of considerations that need to be taken into account to produce 3D printed hollow and thin-walled structures via FDM technique including FDM processing parameters, filament material as well as topology design of the part. The quality of the final 3D printed part is severely influenced by the FDM processing parameters settings, including layer height, infill density, print speed, nozzle temperature, bed temperature, and cooling settings [15]. A study by [16] shows the examined parts printed by AM with the mechanical strength of components with various interior filling percentages. They discovered that the greater the mechanical qualities, the more resistant the part is, and the higher the infill %. From the perspective of multifactor optimisation, it has been determined that infill density 100%; infill angle 45°; and infill speed 90 mm/s are the best printing conditions [17]. For a sample with the best comprehensive mechanical properties, the layer height should be 0.15 mm, the filling density should be 100%, and the printing speed should be 30 mm/s [18]. [19] demonstrated that the mechanical characteristics (maximum failure load) of the samples improved as the layer thickness grew. More than 1000 N could be withstood by the optimised printed Br-PLA specimen with a layer thickness of 0.25 mm, 15.20 infill percentage, and an extruder temperature of 222.82°C. It was found that the hell layer and layer thickness are the parameters that have the biggest effects on the FDM manufactured cubes. With the addition of mass, both of these characteristics subsequently improve the FDM produced cubes' compressive strength [20]. The findings of the investigation make it clear that the orientation of the item during printing has the biggest impact on the final strength. Samples printed XY have the highest tensile strength relative to the component's orientation, while samples printed vertically in the XZ plane have the lowest tensile strength [21].

On the other hand, the success of printing hollow and thin-walled structures can also be influenced by the filament material selection. The walls and general part quality can suffer because some materials are more likely to distort or have poor adherence. The final 3D printed part's quality and robustness are also influenced by the filament material used in FDM technology. The strength, durability, and flexibility of various materials can be significant determinants for selecting the best filament for a part [22]. PLA as an example, has shown to have a good strength compared to another existing materials such as ABS as founded by [23]. As reported by [24], PLA has demonstrated to have good flexural modulus, improved tensility, and greater flexural strengths in its semi-crystalline state. Although PLA has more friction when compared to ABS and is consequently vulnerable to extrusion blockage, it is tougher than ABS [25]. Most 3D printer users select PLA because adhesion between the print and the platform does not necessarily require a hot bed. However, printing with graphene-doped PLA on non-heated build plates is very difficult and difficult to get good prints from [26].

Recognizing that improper FDM processing parameter setting, inappropriate filament material selection, poor part design and topology, could have a negative impact on the final mechanical properties or aesthetic appearance of the 3D printed part, it is crucial to effectively control all the influencing factors to improve the quality characteristics of the final 3D printed part, which in this case is hollow and thin-walled structures. The trials and error process must be replaced immediately with a quick and trustworthy optimization methodology. In this study, one of the most efficient

optimization methods was suggested to optimize the FDM processing parameters and topology design, especially for hollow and thin-walled structures. The integration of Taguchi method and Grey Relational Analysis (GRA) was proposed as comprehensive multi-responses optimization in this study.

The suggested approach allows for time savings, the creation of ideal process conditions, and parameter optimization while staying within set parameters. Thus, the present study deals with establishing a relationship between part and topology design with various FDM processing parameters including layer height, infill density, infill layer thickness, infill flow, infill pattern, printing speed, printing temperature, bed temperature and orientation direction for 3D printed hollow and thin-walled structures. The aims of this study are to identify the optimal topology design, wall thickness and FDM processing parameters as well as the significant factors that influencing the mechanical properties of the 3D printed hollow and thin-walled structures via integration of Taguchi method and GRA.

2. Materials and method

2.1 Raw Materials

PLA was used as the material for the 3D printed hollow and thin-walled structures in this study. The PLA granules were purchased from Shenzhen PioCreat 3D Technology Co., China. The general characteristics of pure PLA granules are listed in Table 2.

Table 2
General properties of Polylactic Acid

Properties	Values
Density (g/cm^3 at 21.5℃)	1.15 ~ 1.22 g/cm^3
Glass transition temperature (℃)	50-60
Melt index (g/10 min)	3-5
Tensile strength (MPa)	32.2 ± 1.3
Impact strength (KJ/m^2)	14.1 ± 1.1

2.2 Implementation of the Taguchi Method and GRA Optimization Procedures

The entire methodology flow chart of the Taguchi method and GRA process optimization method for 3D printed hollow and thin-walled structures in this study is summarized and illustrated in Figure 1.

2.2.1 Determination of quality characteristics

In this paper, the hollow and thin-walled structures was the studied part that produced by FDM technique. Hollow structures are objects or components that have empty or void spaces within them, surrounded by walls or shells. These voids can vary in shape and size, from simple cylindrical tubes to intricate geometries. Hollow structures are designed to reduce weight, improve buoyancy, or house other components, such as wires, fluids, or gases. Meanwhile, thin-walled structures refer to parts with walls that are relatively thin compared to their overall dimensions. The walls can be uniformly thin or have variations in thickness. Thin-walled structures on the other hand, are designed to achieve specific mechanical or thermal properties while minimizing material usage and weight. One of the primary reasons for using hollow and thin-walled structures is to reduce weight. Hollow and thin-walled structures can achieve high strength-to-weight ratios, making them ideal for applications where structural integrity is crucial. Hence, determine the structural strength of hollow

and thin-walled structures under compressive loads is essential for understanding the load-bearing capacity of the parts and ensuring the structures can withstand the forces they are subjected to in real-world applications. This is critical in aerospace, automotive, and transportation industries, where lightweight components with high structural strength led to improved fuel efficiency, faster acceleration, and enhanced overall performance. As in this project, multi-quality characteristics of compression properties for the 3D printed hollow and thin-walled structures including maximum force, maximum stress, maximum strain, and compressive modulus were selected.

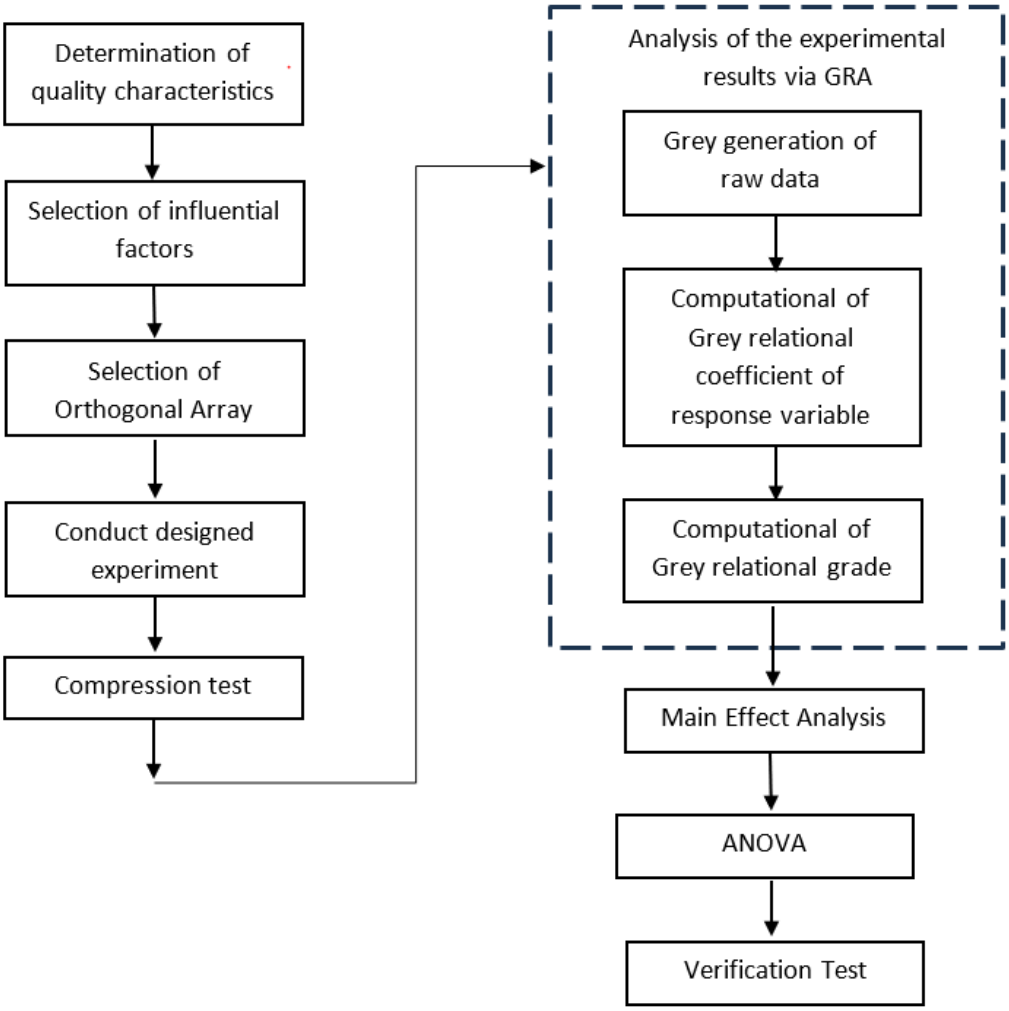

Fig. 1. Methodology process flowchart

2.2.2 Selection of influential factors

The influential factors investigated in this study were topology design, wall thickness and various FDM processing parameters including layer height, infill density, infill layer thickness, infill flow, infill pattern, printing speed, printing temperature, bed temperature and orientation direction at three different levels. Table 3 displays the selected influential factors and their corresponding levels.

As illustrated in Figure 2, three different topological cell designs in the shapes of triangles, squares, and hexagons were chosen for topology design assigned as factor A (refer Table 3). Each construction had a hollow interior with a hollow diameter of 8 mm and a height of 30 mm. The dimension of the hollow and thin-walled structures is 50 mm in length, 50 mm in width, and 30 mm

in height overall. This study also investigated three different wall thickness: 1 mm, 2 mm, and 3 mm accordingly for the hollow and thin-walled structures.

Table 3
Influential factors and levels

Column	Factors	Level 1	Level 2	Level 3
A	Topology design	Triangular	Square	Hexagonal
B	Wall thickness (mm)	1	2	3
C	Layer height (mm)	0.2	0.3	0.4
D	Infill density (%)	20	50	70
E	Infill layer thickness (mm)	0.4	0.6	0.8
F	Infill flow (%)	80	90	100
G	Infill pattern	Octets	Gyroids	Triangles
H	Printing speed (mm/s)	60	80	100
I	Printing temperature (℃)	200	210	220
J	Bed temperature (℃)	65	70	75
K	Orientation direction	Flat along y-axis	Flat along x-axis	45 degrees

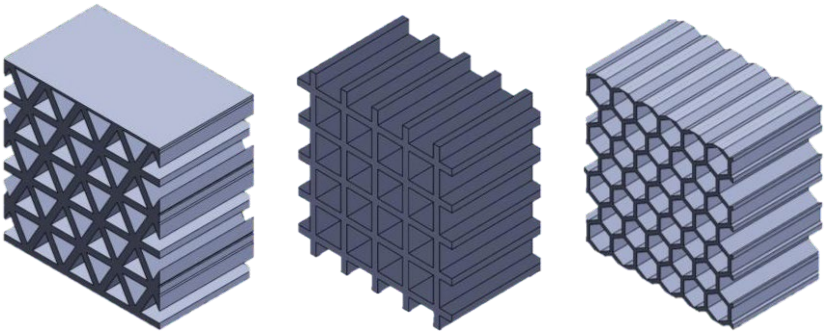

(a) (b) (c)

Fig. 2. Specific topological cell designs of (a) triangular, (b) square and (c) hexagonal for hollow and thin-walled structures in 3D

2.2.3 Selection of Taguchi's orthogonal array (OA)

Selection of an appropriate OA was based on the total degree of freedom (DOF) of the overall influential factors as in Table 4. Considering eleven factors each at three levels, the total DOF required for the experiment is 22 DOF (DOF = number of levels – 1). The total DOF of selected OA must be greater than or equal to the total DOF required for the experiment. Hence, L^{27} OA having 26 DOF was chosen for this study because it is the lowest order array that can accommodate all the influential factors as shown in Table 4.

Table 4
L^{27} OA

Trial	Factors										
No.	A	B	C	D	E	F	G	H	I	J	K
1	1	1	1	1	1	1	1	1	1	1	1
2	1	1	1	1	2	2	2	2	2	2	2
3	1	1	1	1	3	3	3	3	3	3	3
4	1	2	2	2	1	1	1	2	2	2	3
5	1	2	2	2	2	2	2	3	3	3	1
6	1	2	2	2	3	3	3	1	1	1	2
7	1	3	3	3	1	1	1	3	3	3	2
8	1	3	3	3	2	2	2	1	1	1	3
9	1	3	3	3	3	3	3	2	2	2	1
10	2	1	2	3	1	2	3	1	2	3	1
11	2	1	2	3	2	3	1	2	3	1	2
12	2	1	2	3	3	1	2	3	1	2	3
13	2	2	3	1	1	2	3	2	3	1	3
14	2	2	3	1	2	3	1	3	1	2	1
15	2	2	3	1	3	1	2	1	2	3	2
16	2	3	1	2	1	2	3	3	1	2	2
17	2	3	1	2	2	3	1	1	2	3	3
18	2	3	1	2	3	1	2	2	3	1	1
19	3	1	3	2	1	3	2	1	3	2	1
20	3	1	3	2	2	1	3	2	1	3	2
21	3	1	3	2	3	2	1	3	2	1	3
22	3	2	1	3	1	3	2	2	1	3	3
23	3	2	1	3	2	1	3	3	2	1	1
24	3	2	1	3	3	2	1	1	3	2	2
25	3	3	2	1	1	3	2	3	2	1	2
26	3	3	2	1	2	1	3	1	3	2	3
27	3	3	2	1	3	2	1	2	1	3	1

2.2.4 Compression test

The 3D printed hollow and thin-walled structures have been subjected to a compression test using the ASTM D695 standard methodology (Figure 3). Using a 250kN SHIMADZU universal testing equipment, the test was run at 2mm/min velocity. To ensure the accuracy of the findings, three samples were examined for each trial. Grey relational analysis (GRA) was used to analyse the experimental data.

Fig. 3. Compression testing on 3D printed hollow and thin-walled structures

3. Results and discussion

3.1 Analysis of the Experimental Results via Grey Relational Analysis GRA

The Grey System Theory (GST), developed by Deng, is a decision-making methodology that employs the terms black and white to indicate systems with limited data and systems with complete data, respectively. A grey relation is utilized to characterize the distance between two components, and the incomplete information is used to indicate the degree of link between two sequences. When the experiment is unclear or the experimental design is flawed, gradient augmentation makes up for the absence of statistical regression. While the Taguchi methodology is not appropriate for optimizing multiple responses, GRA is a great way to study correlations between sequences with fewer data in order to solve the drawbacks of statistical methods [27]. This issue can be resolved through GRA. Integration of GRA and Taguchi method can be used to optimise a variety of attribute features and look into relationships of each factor [28]. GRA determines the Grey Relational Grade (GRG) to assess a large number of responses. It is possible to optimise several responses by optimising a single GRG [29].

3.1.1 Grey generation of raw data

To prepare the raw data for the analysis, where the original sequence is translated to a comparable sequence, the first step GRA is normalization of the compression data. In this study, the raw data of the compression test including maximum force, maximum stress, maximum strain, and compressive modulus were normalized between zero and unity. Table 5 is first normalized according to the-"larger-the-better" characteristic of the sequence by using Eq. (1). Table 4 lists all the normalization data for maximum force, maximum stress, maximum strain, and compressive modulus for the 3D printed hollow and thin-walled structures for each trial.

$$x_i^*(k) = \frac{x_i^*(k) - min\, x_i^0(k)}{max\, x_i^0(k) - min\, x_i^0(k)} \quad (1)$$

Table 5
Normalization of maximum force, maximum stress, maximum strain, and compressive modulus

Trial No	Max force	Max Stress	Max Strain	Compressive Modulus
1	0.3813	0.3654	0.1065	0.4453
2	0.4131	0.4037	0.1144	0.4606
3	0.3688	0.3824	0.0555	0.5562
4	0.6388	0.6540	0.2746	0.4247
5	0.6591	0.6694	0.3364	0.3717
6	0.6990	0.7148	0.2915	0.4422
7	0.5148	0.5218	1.0000	0.0000
8	0.7967	0.7990	0.9995	0.0812
9	0.8241	0.8127	0.5414	0.2791
10	0.0439	0.0403	0.0508	0.2077
11	0.0036	0.0029	0.0233	0.2019
12	0.0000	0.0000	0.0446	0.1692
13	0.4410	0.4485	0.1515	0.4380
14	0.4531	0.4583	0.1699	0.4210
15	0.4087	0.4235	0.1169	0.4833
16	0.4467	0.4510	0.4240	0.3028
17	0.3351	0.3429	0.1740	0.3215
18	0.0383	0.0499	0.3603	0.0344
19	0.4376	0.4171	0.0772	0.5429
20	0.4759	0.4554	0.0986	0.5361
21	0.3840	0.3644	0.0936	0.4596
22	1.0000	1.0000	0.1955	0.7933
23	0.9845	0.9824	0.1093	1.0000
24	0.9362	0.9287	0.1863	0.7602
25	0.2575	0.2644	0.0000	0.5539
26	0.2524	0.2558	0.0275	0.4926
27	0.2954	0.2975	0.0082	0.5744

3.1.2 Determination of deviation sequence

The deviation sequence $\Delta 0_i\,(k)$ is the absolute difference between the reference sequence $x_0{*}\,(k)$ and the comparability sequence $x_i{*}\,(k)$ after normalization. It is determined using Eq. (2) and listed in Table 6.

$$\Delta 0_i\,(k) = |x_0^*\,(k) - x_1^*\,(k)| \tag{2}$$

Table 6
Deviation Sequence

Trial No	Max force	Max Stress	Max Strain	Compressive Modulus
1	0.6187	0.6346	0.8935	0.5547
2	0.5869	0.5963	0.8856	0.5394
3	0.6312	0.6176	0.9445	0.4438
4	0.3612	0.3460	0.7254	0.5753
5	0.3409	0.3306	0.6636	0.6283
6	0.3010	0.2852	0.7085	0.5578
7	0.4852	0.4782	0.0000	1.0000
8	0.2033	0.2010	0.0005	0.9188
9	0.1759	0.1873	0.4586	0.7209
10	0.9561	0.9597	0.9492	0.7923
11	0.9964	0.9971	0.9767	0.7981
12	1.0000	1.0000	0.9554	0.8308
13	0.5590	0.5515	0.8485	0.5620
14	0.5469	0.5417	0.8301	0.5790
15	0.5913	0.5765	0.8831	0.5167
16	0.5533	0.5490	0.5760	0.6972
17	0.6649	0.6571	0.8260	0.6785
18	0.9617	0.9501	0.6397	0.9656
19	0.5624	0.5829	0.9228	0.4571
20	0.5241	0.5446	0.9014	0.4639
21	0.6160	0.6356	0.9064	0.5404
22	0.0000	0.0000	0.8045	0.2067
23	0.0155	0.0176	0.8907	0.0000
24	0.0638	0.0713	0.8137	0.2398
25	0.7425	0.7356	1.0000	0.4461
26	0.7476	0.7442	0.9725	0.5074
27	0.7046	0.7025	0.9918	0.4256

3.1.3 Determination of Grey Relational Coefficient (GRC) and Grey Relational Grade (GRG)

The relationship between the ideal (optimal) and actual normalized maximum force, maximum stress, maximum strain, and compressive modulus is expressed by GRC for all sequences. If the two sequences agree at all points, then their GRC is 1. The GRC $\gamma\big(x_0(k), x_i(k)\big)$ as expressed by Eq. (3).

$$\gamma\big(x_0(k), x_i(k)\big) = \frac{\Delta_{min} + \zeta\Delta_{max}}{\Delta_{0i}\,(k) + \zeta\Delta_{max}} \tag{3}$$

where, Δ_{min} is the smallest value of $\Delta 0_i\,(k) = \; min_{\,i}\, min_k\, |x_0^*\,(k) - x_1^*\,(k)|$ and Δ_{max} is the largest value of $\Delta 0_i\,(k) = \; max_{\,i}\, max_k\, |x_0^*\,(k) - x_1^*\,(k)|$, $x_0^*\,(k)$ is the ideal normalized maximum force, maximum stress, maximum strain and compressive modulus, $x_1^*\,(k)$ is the normalized comparability sequence, and ζ is the distinguishing coefficient. The value of ζ can be adjusted with the systematic actual need and defined in the range between 0 and 1; here it is chosen as 0.5.

The GRG provides the foundation for the overall assessment of the many performance aspects. The GRG, which is defined as the average of the GRC, is shown in Eq. (4). Table 7 shows the results of GRC and GRG.

$$\gamma\,\big(x_{0,} x_i\big) = \frac{1}{m}\sum_{i=1}^{m}\gamma\big(x_0(k), x_i(k)\big) \tag{4}$$

Table 7
Grey Relational Coefficient (GRC) and Grey Relational Grade (GRG)

Trial No	Max force	Max Stress	Max Strain	Compressive Modulus	GRG
1	0.1117	0.4407	0.3588	0.4741	0.3463
2	0.4600	0.4561	0.3608	0.4811	0.4395
3	0.4420	0.4474	0.3461	0.5298	0.4413
4	0.5806	0.5910	0.4080	0.4650	0.5112
5	0.5946	0.6019	0.4297	0.4431	0.5173
6	0.6242	0.6368	0.4137	0.4727	0.5368
7	0.5075	0.5112	1.0000	0.3333	0.5880
8	0.7109	0.7133	0.9991	0.3524	0.6939
9	0.7398	0.7275	0.5216	0.4095	0.5996
10	0.3434	0.3425	0.3450	0.3869	0.3545
11	0.3341	0.3340	0.3386	0.3852	0.3480
12	0.3333	0.3333	0.3435	0.3757	0.3465
13	0.4721	0.4755	0.3708	0.4708	0.4473
14	0.4776	0.4800	0.3759	0.4634	0.4492
15	0.4582	0.4645	0.3615	0.4918	0.4440
16	0.4747	0.4766	0.4647	0.4176	0.4584
17	0.4292	0.4321	0.3771	0.4243	0.4157
18	0.3421	0.3448	0.4387	0.3411	0.3667
19	0.4706	0.4617	0.3514	0.5224	0.4515
20	0.4882	0.4787	0.3568	0.5187	0.4606
21	0.4480	0.4403	0.3555	0.4806	0.4311
22	1.0000	1.0000	0.3833	0.7075	0.7727
23	0.9699	0.9660	0.3595	1.0000	0.8239
24	0.8868	0.8751	0.3806	0.6759	0.7046
25	0.4024	0.4047	0.3333	0.5285	0.4172
26	0.4008	0.4019	0.3396	0.4963	0.4096
27	0.4151	0.4158	0.3352	0.5402	0.4266

3.2 Determination of Optimal Factors via Main Effect Analysis

To determine the optimal combination of each factor including topology design, wall thickness and various FDM processing parameters (layer height, infill density, infill layer thickness, infill flow, infill pattern, printing speed, printing temperature, bed temperature and orientation direction) for the 3D printed hollow and thin-walled structures, the average GRG for each factors level was calculated by employing the main effect analysis of the Taguchi method. This process is performed by sorting the GRG corresponding to the levels of the topology design, wall thickness and various FDM processing parameters in each column of the OA and then taking the average of each factor with the same levels. Figure 4 displays the main effect analysis graph from the value of GRG.

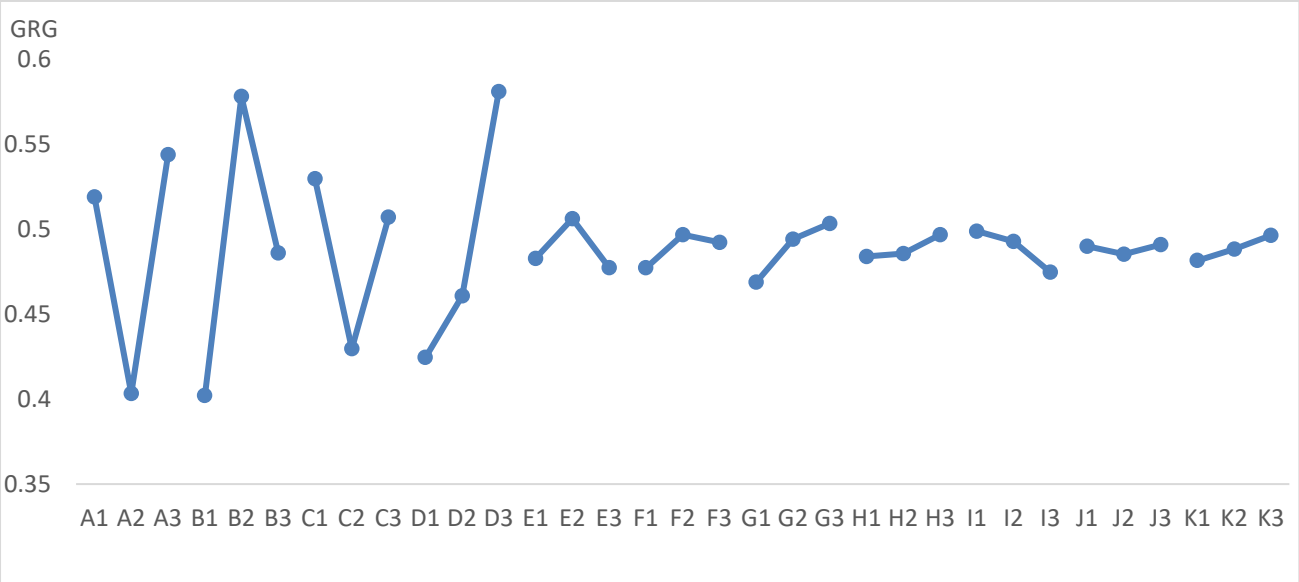

Fig. 4. Graph display of Main Effect Analysis

Figure 4 clearly shows that the multiple quality characteristics represent in GRG (y axis) which in this case are maximum force, maximum stress, maximum strain, and compressive modulus of the PLA 3D printed hollow and thin-walled structures are significantly affected by the adjustments of the influential factors (the horizontal axis). The influential factors in this study including topology design, wall thickness and various FDM processing parameters (layer height, infill density, infill layer thickness, infill flow, infill pattern, printing speed, printing temperature, bed temperature and orientation direction). Referring to Figure 4, the line graph displays the remarkable trend in certain factors such as topology designs (assigned as factor A), wall thickness (assigned as factor B), layer height (assigned as factor C) as well as infill density (assigned as factor D).

The different topology designs as in this case are triangular, square, and hexagonal have a significant impact on the maximum force, maximum stress, maximum strain, and compressive modulus of the PLA 3D printed hollow and thin-walled structures. Hexagonal topology design (assigned as A3) depicted the highest GRG as can be seen in Figure 4. Considering that the GRG represents the level of correlation between the reference and comparability sequences, a larger GRG indicates that the comparability sequence exhibits a stronger correlation with the reference sequence. A larger GRG results in better multiple quality characteristics which in this case are maximum force, maximum stress, maximum strain, and compressive modulus of the PLA 3D printed hollow and thin-walled structures. Hexagonal topology design most likely honeycomb shape structures provide excellent strength-to-weight ratios. The inherent geometry distributes material efficiently, resulting in lightweight components. The interconnected cells create a lattice-like framework that disperses loads evenly throughout the structure, enhancing its ability to withstand forces, including compression [30]. This is especially crucial in applications like aerospace and automotive, where lightweight components improve fuel efficiency and overall performance.

The choice of wall thickness in hollow and thin-walled structures in 3D printing on the other hand, can have a significant impact on the performance, functionality, and aesthetics of the printed object. Different wall thicknesses serve specific purposes and affect various aspects of the final 3D printed part [31]. Referring to Figure 4, B2 which is wall thickness of 2 mm showed the highest GRG. Thicker walls generally provide greater structural strength and integrity. They can withstand higher loads and are less likely to deform or fail under stress. This is important in applications where structural stability is critical, such as load-bearing components in machinery or infrastructure. Meanwhile, for layer

height, C1 which is layer height of 0.2 mm demonstrated the highest value of GRG. Layer height in 3D printing refers to the vertical distance or thickness of each individual layer that makes up a 3D-printed part. It is one of the critical parameters in the 3D printing process and directly affects the quality, resolution, and appearance of the final print. Smaller layer heights result in finer details and smoother surface finishes and also can provide improved dimensional accuracy and finer tolerances. In contrast, thicker layers may provide better layer-to-layer adhesion and greater strength in the z-axis (vertical direction). This can be beneficial for structural components that need to withstand vertical loads [32].

From Figure 4, the GRG values also show substantial increase in the increment of infill density percentage. Assigned as factor D, infill density in 3D printing refers to the internal structure or lattice pattern used to fill the empty space within a hollow or thin-walled part. D3, which is 70% of infill density shows the highest value of GRG. Higher infill densities provide greater structural strength and rigidity to the 3D-printed object. This is crucial for load-bearing or structural components where strength and stability are paramount [33]. For another factor such as infill layer thickness, infill flow, infill pattern, printing speed, printing temperature, bed temperature and orientation direction, the adjustment of these factors demonstrates lack of significant towards GRG values.

In this case, the best combination of influential factors and levels can easily be obtained from the main effect analysis by selecting the level of each factor with the highest GRG. Table 8 listed the optimal factors for PLA 3D printed hollow and thin-walled structures in this study.

Table 8
Optimal factors

Optimal Factor		
A3	Topology design	Hexagonal
B2	Wall thickness (mm)	2
C1	Layer height (mm)	0.2
D3	Infill density (%)	70
E2	Infill layer thickness (mm)	0.6
F1	Infill flow (%)	80
G3	Infill pattern	Triangles
H3	Printing speed (mm/s)	100
I2	Printing temperature (℃)	210
J1	Bed temperature (℃)	65
K1	Orientation direction	Y axis

3.3 Analysis of Variance (ANOVA)

To examine the extent in which influential factors including topology design, wall thickness and various FDM processing parameters (layer height, infill density, infill layer thickness, infill flow, infill pattern, printing speed, printing temperature, bed temperature and orientation direction) significantly influence the maximum force, maximum stress, maximum strain and compressive modulus of the PLA 3D printed hollow and thin-walled structures, ANOVA is performed on the Taguchi method for the GRG of 27 comparability sequences (Table 7). The computed quantity of degrees of freedom (DOF), sum of square, variance, F-ratio, and percentage contribution (%) are presented in Table 9.

Table 9
ANOVA

Column	Parameter	DOF	Sum Square	Variance	F-Ratio	%
A	Topology design	2	0.1017	0.0509	357.7401	23.2443
B	Wall thickness	2	0.1402	0.0701	492.8816	32.0251
C	Layer height	2	0.0497	0.0248	174.6415	11.3474
D	Infill Density	2	0.1211	0.0605	425.7391	27.6625
E	Infill layer thickness	2	0.0042	0.0021	14.9405	0.9708
F	Infill flow	2	0.0019	0.0009	6.6641	0.4330
G	Infill pattern	2	0.0058	0.0029	20.3442	1.3219
H	Printing speed	2	0.0009	0.0004	3.1065	0.2018
I	Printing temperature	2	0.0028	0.0014	9.9246	0.6449
J	Bed temperature	2	0.0002	0.0001	0.5634	0.0366
K	Orientation direction	2	0.0010	0.0005	3.5014	0.2275
	ERROR	58	0.0082	0.0001		1.8843
	TOTAL	80	0.4376			100

The significance of each factor can be determined by the percentage contribution. The 10% rule, according to which a factor is deemed negligible if its influence is less than 10% of the largest factor influence, was proposed as an alternative by [34]. From the results of ANOVA in Table 9, wall thickness appears to be the most significant factor affecting the compression properties of the hollow and thin-walled 3D-printed structures with the highest percentage contribution of 32.025%, thus outweighing the other factors. The result is consistent with what was reported by [35], who found that the compressive strength of the 3D-printed PLA samples increased as the wall thickness increased. The ANOVA also reveals that infill density, topology design, and layer height are significant because their percentages are more than 10% of the highest factor (32.025%) with the percentage contribution of 27.663%, 23.244%, and 11.347% respectively. Meanwhile, other factors such as infill layer thickness, infill flow, infill pattern, printing speed, printing temperature, bed temperature and orientation direction significantly are less than 10% of the highest factor influence, thus considered insignificant.

3.4 Verification Test

Once the optimal levels of the influential factors which in this case are topology design, wall thickness and various FDM processing parameters (layer height, infill density, infill layer thickness, infill flow, infill pattern, printing speed, printing temperature, bed temperature and orientation direction) are identified, the subsequent step is to verify the improvements in the quality characteristics by using this optimal combination. The verification test can be used to assess the accuracy of the integration of Taguchi method and GRA. An experimental verification test is conducted by using the same procedures as previous runs under the optimal factor conditions, namely, A3, B2, C1, D3, E2, F1, G3, H3, I2, J1 and K1 (refer Table 7) to produce optimize PLA 3D printed hollow and thin-walled structures. Table 10 shows the maximum force, maximum stress, maximum strain, and compressive modulus of the optimized PLA 3D printed hollow and thin-walled structures. The comparison of the maximum force, maximum stress, maximum strain, and compressive modulus of the hollow and thin-walled 3D-printed structures before optimization and after optimization are presented in Table 11.

Table 10
Compression test results from optimized factors

Sample	Max force (N)	Max Stress (N/mm2)	Max Strain (%)	Compressive Modulus (E)
1	47509.20	31.67	14.32	2.21
2	37116.40	24.74	16.96	1.46
3	41448.80	27.63	15.02	1.84
Average	42024.80	28.02	15.43	1.84

Table 11
Verification test results comparison

	Max Force (N)	Max Stress (N/m^2)	Max Strain	Compression Modulus (MPa)
Before Optimization	36006.80	14.02	15.72	0.90
After Optimization	42024.80	28.02	15.43	1.84
Difference	15.42%	66.62%	-1.88%	68.61%

Referring to Table 11, after a thorough optimization process via integration of Taguchi method and GRA, the compression properties of the hollow and thin-walled 3D-printed structures have undergone remarkable improvements. The percentage differences between the three quality characteristics for maximum force, maximum strength and compression strength was found to be greatly improved to 15.42%, 66.62% and 68.61% respectively. The maximum force has been significantly enhanced, now reaching 42024.80 N after optimization process compared to 36006.80 N before optimization. Additionally, the maximum stress and compression modulus for the hollow and thin-walled 3D-printed structures have been boosted to 28.02 N/m2 and 1.84 MPa, accordingly after the optimization.

The enhancement in maximum force and maximum stress means that for the part can withstand higher loads before failure. A higher compression modulus indicates that the part is less prone to deformation when subjected to compressive loads. In the context of 3D printed hollow and thin-walled structures, this means that the walls of the structures will maintain their shape and structural integrity even under heavy compression. With improved compression properties, the structures can handle more significant external forces, making them more robust and reliable.

4. Conclusions

In conclusion, the integration of the Taguchi Method and Grey Relational Analysis (GRA) has proven to be a prevailing and effective approach for the optimization of both the topology and mechanical properties of 3D printed hollow and thin-walled structures. This innovative methodology has enabled to achieve remarkable advancements in the design and performance of such structures, with wide-ranging implications for various industries and applications. From the findings in main effects analysis, the optimized factors for the 3D printed hollow and thin-walled structures were identified as topology design (hexagonal), wall thickness (2 mm), layer height (0.2 mm), infill density (20%), infill layer thickness (0.6 mm), infill flow (80%), infill pattern (Triangle), print speed (100 mm/s), printing temperature (210°C), bed temperature (65°C), and orientation direction (flat along the Y-axis). Meanwhile, from ANOVA, wall thickness appears to be the most significant factor affecting the compression properties of the hollow and thin-walled 3D-printed structures with the highest percentage contribution of 32.025%, thus outweighing the other factors. The study also indicated that maximum force, maximum stress, and compression strength has been greatly enhanced to up to 15.42%, 66.62% and 68.61% accordingly after the optimization process via integration of the

Taguchi Method and GRA. Integrating both Taguchi method and GRA has the potential to improve multi-response performance where the number of samples or tests can be reduced thus minimizing the cost of production and testing. The application of the Taguchi Method allowed us to efficiently explore a wide parameter space and pinpoint key variables for optimization. GRA on the other hand enabled to assess the relationships between multi-quality characteristics for the part as in this case are topology design, wall thickness and various FDM processing parameters (layer height, infill density, infill layer thickness, infill flow, infill pattern, printing speed, printing temperature, bed temperature and orientation direction) with desired mechanical properties, providing a comprehensive understanding of the complex system. The results of this study not only contribute to advancements in 3D printing technology but also offer practical implications in various industries, from aerospace and automotive engineering to healthcare and beyond. The ability to create lightweight yet robust structures align with the ongoing pursuit of efficiency, sustainability, and cost-effectiveness in product design and manufacturing as 3DP technologies are developing quickly and demands for specialized materials to fulfill the required properties of end parts of products.

Acknowledgement

This research was supported by Ministry of Higher Education Malaysia (MOHE) through Fundamental Research Grant Scheme (FRGS/1/2021/TKO/UNIMAP/02/43).

References

[1] Shahrubudin, Nurhalida, Te Chuan Lee, and R. J. P. M. Ramlan. "An overview on 3D printing technology: Technological, materials, and applications." *Procedia Manufacturing* 35 (2019): 1286-1296. https://doi.org/10.1016/j.promfg.2019.06.089

[2] Keleş, Özgür, Caleb Wayne Blevins, and Keith J. Bowman. "Effect of build orientation on the mechanical reliability of 3D printed ABS." *Rapid Prototyping Journal* 23, no. 2 (2017): 320-328. https://doi.org/10.1108/RPJ-09-2015-0122

[3] Sood, Anoop K., Raj K. Ohdar, and Siba S. Mahapatra. "Experimental investigation and empirical modelling of FDM process for compressive strength improvement." *Journal of Advanced Research* 3, no. 1 (2012): 81-90. https://doi.org/10.1016/j.jare.2011.05.001

[4] Low, Ze-Xian, Yen Thien Chua, Brian Michael Ray, Davide Mattia, Ian Saxley Metcalfe, and Darrell Alec Patterson. "Perspective on 3D printing of separation membranes and comparison to related unconventional fabrication techniques." *Journal of membrane science* 523 (2017): 596-613. https://doi.org/10.1016/j.memsci.2016.10.006

[5] Sniderman, B., P. Baum, and V. Rajan. "3D opportunity for life: Additive manufacturing takes humanitarian action." *Deloitte Rev. Available online: https://www2.deloitte.com/insights/us/en/deloitte-review/issue-19/3d-printing-for-humanitarian-action. html (accessed on 12 October 2017)* (2016).

[6] Huang, Samuel H., Peng Liu, Abhiram Mokasdar, and Liang Hou. "Additive manufacturing and its societal impact: a literature review." *The International journal of advanced manufacturing technology* 67 (2013): 1191-1203. https://doi.org/10.1007/s00170-012-4558-5

[7] Stansbury, Jeffrey W., and Mike J. Idacavage. "3D printing with polymers: Challenges among expanding options and opportunities." *Dental materials* 32, no. 1 (2016): 54-64. DOI: 10.1016/j.dental.2015.09.018

[8] Singh, Balwant, Raman Kumar, and Jasgurpreet Singh Chohan. "Multi-objective optimization of 3D Printing process using genetic algorithm for fabrication of copper reinforced ABS parts." *Materials Today: Proceedings* 48 (2022): 981-988. https://doi.org/10.1016/j.matpr.2021.06.264

[9] Kamio, Takashi, and Takeshi Onda. "Fused deposition modeling 3D printing in oral and maxillofacial surgery: problems and solutions." *Cureus* 14, no. 9 (2022). DOI: 10.7759/cureus.28906

[10] Joseph, Tomy Muringayil, Anoop Kallingal, Akshay Maniyeri Suresh, Debarshi Kar Mahapatra, Mohamed S. Hasanin, Józef Haponiuk, and Sabu Thomas. "3D printing of polylactic acid: recent advances and opportunities." *The International Journal of Advanced Manufacturing Technology* 125, no. 3-4 (2023): 1015-1035. https://doi.org/10.1007/s00170-022-10795-y

[11] Camargo, José C., Álisson R. Machado, Erica C. Almeida, and Erickson Fabiano Moura Sousa Silva. "Mechanical properties of PLA-graphene filament for FDM 3D printing." *The International Journal of Advanced Manufacturing Technology* 103 (2019): 2423-2443. https://doi.org/10.1007/s00170-019-03532-5
[12] Mayekar, Pooja C., Wanwarang Limsukon, Anibal Bher, and Rafael Auras. "Breaking It Down: How Thermoplastic Starch Enhances Poly (lactic acid) Biodegradation in Compost– A Comparative Analysis of Reactive Blends." *ACS Sustainable Chemistry & Engineering* (2023). https://doi.org/10.1021/acssuschemeng.3c01676
[13] Kasmi, Samir, Julien Cayuela, Bertrand De Backer, Eric Labbé, and Sébastien Alix. "Modified polylactic acid with improved impact resistance in the presence of a thermoplastic elastomer and the influence of fused filament fabrication on its physical properties." *Journal of Composites Science* 5, no. 9 (2021): https://doi.org/10.3390/jcs5090232
[14] Chen, Yonglin, Junming Zhang, Zefu Li, Huliang Zhang, Jiping Chen, Weidong Yang, Tao Yu, Weiping Liu, and Yan Li. "Manufacturing Technology of Lightweight Fiber-Reinforced Composite Structures in Aerospace: Current Situation and toward Intellectualization." *Aerospace* 10, no. 3 (2023): https://doi.org/10.3390/aerospace10030206
[15] Dey, Arup, and Nita Yodo. "A systematic survey of FDM process parameter optimization and their influence on part characteristics." *Journal of Manufacturing and Materials Processing* 3, no. 3 (2019): 64. DOI: 10.3390/jmmp3030064
[16] Mensah, Rhoda Afriyie, David Aronsson Edström, Oskar Lundberg, Vigneshwaran Shanmugam, Lin Jiang, Xu Qiang, Michael Försth, Gabriel Sas, Mikael Hedenqvist, and Oisik Das. "The effect of infill density on the fire properties of polylactic acid 3D printed parts: A short communication." *Polymer testing* 111 (2022): https://doi.org/10.1016/j.polymertesting.2022.107594
[17] Kumar, Sudhir, Rupinder Singh, T. P. Singh, and Ajay Batish. "On flexural and pull out properties of 3D printed PLA based hybrid composite matrix." *Materials Research Express* 7, no. 1 (2020): 015330. DOI: 10.1088/2053-1591/ab66f4
[18] Yu, Zhu, Yingchao Gao, Jie Jiang, Hai Gu, Shuaishuai Lv, Hongjun Ni, Xingxing Wang, and Chaofan Jia. "Study on effects of FDM 3D printing parameters on mechanical properties of polylactic acid." In *IOP Conference Series: Materials Science and Engineering*, vol. 688, no. 3, p. 033026. IOP Publishing, 2019. DOI: 10.1088/1757-899X/688/3/033026
[19] Ferretti, Patrich, Christian Leon-Cardenas, Gian Maria Santi, Merve Sali, Elisa Ciotti, Leonardo Frizziero, Giampiero Donnici, and Alfredo Liverani. "Relationship between FDM 3D printing parameters study: parameter optimization for lower defects." *Polymers* 13, no. 13 (2021): 2190. https://doi.org/10.3390/polym13132190
[20] Rosli, Nur Ameelia, Rafidah Hasan, and Mohd Rizal Alkahari. "Effect of default parameters on properties of FDM printed cubes." *Proceedings of Mechanical Engineering Research Day* 2018 (2018): 230-232.
[21] Vosynek, Petr, Tomas Navrat, Adela Krejbychova, and David Palousek. "Influence of process parameters of printing on mechanical properties of plastic parts produced by FDM 3D printing technology." In *MATEC web of conferences*, vol. 237, p. 02014. EDP Sciences, 2018. https://doi.org/10.1051/matecconf/201823702014
[22] Getme, Abhijit Sudamrao, and Brijesh Patel. "A review: Bio-fiber's as reinforcement in composites of polylactic acid (PLA)." *Materials Today: Proceedings* 26 (2020): 2116-2122. https://doi.org/10.1016/j.matpr.2020.02.457
[23] Raj, S. Aravind, E. Muthukumaran, and K. Jayakrishna. "A case study of 3D printed PLA and its mechanical properties." *Materials Today: Proceedings* 5, no. 5 (2018): 11219-11226. DOI: 10.1016/j.matpr.2018.01.146
[24] Nagarjun, J., J. Kanchana, G. RajeshKumar, S. Manimaran, and M. Krishnaprakash. "Enhancement of mechanical behavior of PLA matrix using tamarind and date seed micro fillers." *Journal of Natural Fibers* 19, no. 12 (2022): 4662-4674. DOI: 10.1080/15440478.2020.1870616
[25] Liao, Yuhan, Chang Liu, Bartolomeo Coppola, Giuseppina Barra, Luciano Di Maio, Loredana Incarnato, and Khalid Lafdi. "Effect of porosity and crystallinity on 3D printed PLA properties." *Polymers* 11, no. 9 (2019): 1487. DOI: 10.3390/polym11091487
[26] Arockiam, A. Joseph, S. Rajesh, S. Karthikeyan, Senthil Muthu Kumar Thiagamani, R. G. Padmanabhan, Mohamed Hashem, Hassan Fouad, and AbuZar Ansari. "Mechanical and thermal characterization of additive manufactured fish scale powder reinforced PLA biocomposites." *Materials Research Express* 10, no. 7 (2023): DOI: 10.1088/2053-1591/ace41d
[27] Acır, Adem, Mehmet Emin Canlı, İsmail Ata, and Ramazan Çakıroğlu. "Parametric optimization of energy and exergy analyses of a novel solar air heater with grey relational analysis." *Applied Thermal Engineering* 122 (2017): 330-338. https://doi.org/10.1016/j.applthermaleng.2017.05.018
[28] Kumar, Sudhir, Sanjoy Kumar Ghoshal, Pawan Kumar Arora, and Leeladhar Nagdeve. "Multi-variable optimization in die-sinking EDM process of AISI420 stainless steel." *Materials and Manufacturing Processes* 36, no. 5 (2021): 572-582. DOI: 10.1080/10426914.2020.1843678

[29] Raykar, S. J., D. M. D'Addona, and A. M. Mane. "Multi-objective optimization of high speed turning of Al 7075 using grey relational analysis." *Procedia Cirp* 33 (2015): 293-298. https://doi.org/10.1016/j.procir.2015.06.052
[30] Nazir, Aamer, Ahmad Bin Arshad, Shang-Chih Lin, and Jeng-Ywan Jeng. "Mechanical performance of lightweight-designed honeycomb structures fabricated using multijet fusion additive manufacturing technology." *3D Printing and Additive Manufacturing* 9, no. 4 (2022): 311-325. DOI: 10.1089/3dp.2021.0004
[31] Liu, Yanping, Wei Bai, Xian Cheng, Jiehua Tian, Donghao Wei, Yuchun Sun, and Ping Di. "Effects of printing layer thickness on mechanical properties of 3D-printed custom trays." *The Journal of Prosthetic Dentistry* 126, no. 5 (2021): 671-e1. https://doi.org/10.1016/j.prosdent.2020.08.025
[32] Syrlybayev, Daniyar, Beibit Zharylkassyn, Aidana Seisekulova, Mustakhim Akhmetov, Asma Perveen, and Didier Talamona. "Optimisation of strength properties of FDM printed parts—A critical review." *Polymers* 13, no. 10 (2021): 1587. https://doi.org/10.3390/polym13101587
[33] Baechle-Clayton, Maggie, Elizabeth Loos, Mohammad Taheri, and Hossein Taheri. "Failures and flaws in fused deposition modeling (FDM) additively manufactured polymers and composites." *Journal of Composites Science* 6, no. 7 (2022): 202. DOI: 10.3390/jcs6070202
[34] Roy, Ranjit K. *A primer on the Taguchi method*. Society of Manufacturing Engineers, 2010.
[35] Abbas, Jamal A., Ibtisam A. Said, Manaf A. Mohamed, Suhad A. Yasin, Zeravan A. Ali, and Idrees H. Ahmed. "Electrospinning of polyethylene terephthalate (PET) nanofibers: Optimization study using taguchi design of experiment." In *IOP conference series: materials science and engineering*, vol. 454, p. 012130. IOP Publishing, 2018. http://dx.doi.org/10.1088/1757-899X/454/1/012130